Computational Efficiency Assessment of Multi-Period AC Optimal Power Flow including Energy Storage Systems

Salman Zaferanlouei
Magnus Korpås
Jamshid Aghaei
Hossein Farahmand
Department of Electric Power Engineering
Norwegian University of Science and Technology
Trondheim, Norway

Naser Hashemipour
Department of Electrical and electronics engineering
Shiraz University of Technology
Shiraz, Iran

***Abstract*—In this paper, firstly, a formulation for Multi-Period AC Optimal Power Flow is developed to incorporate inter-temporal constraints and, specifically, equations representing energy storage systems. Secondly, a solution method for the resulting optimisation model is proposed based on the primal-dual interior point method and the mathematical details underlying the solution approach are explicitly and extensively elaborated. The developed solver is tested on a simple 3 bus system. Finally, the computationally efficiency is compared with similar GAMS- and MATLAB-based non-linear commercial solvers. The main contributions of our proposed method can be summarised as follows: a) Shorter computational time is observed in the test due to the merit of using analytical differentiation in the solution method rather than numerical, which is typically used by commercial solvers. b) The formulation and solution method provides the basis of an open-box flexible solver that can be extended to include other components of power systems.**

Keywords*—*Multi-Period ACOPF, Interior Point Method, Energy Storage Systems

NOMENCLATURE

General

f, F	Objective function of one time-step and the next horizon
g, G	Vectors of equality constraint in one time-step and over future horizon
h, H	Vectors of inequality constraints in one time-step and over future horizon
$S_{bus,t}$	$n_b \times 1$ Vector of complex bus power injections for one time-step
$[\mathrm{A}]$	Diagonal matrix of vector A located on the diagonal
$V_{di,t}$, $V_{qi,t}$	Real and imaginary part of voltage at bus i and time t
I_{bus}	$n_b \times 1$ Vector of complex bus current injections
S^{fr}, S^{to}	$n_l \times 1$vectors of complex branch power flows, $from$ and to ends
S_g, S_d	$(n_g \times 1)$, $(n_b \times 1)$ Vectors of generator and load complex power injection
$Egrid$, $Igrid$	Equality and Inequality constraints related to grid
$Estorage$, $Istorage$	Equality and Inequality constraints related to storage
$A^\top$	(non-conjugate) transpose of matrix A
A_b	Derivative of vector A w.r.t variable b
A^*	Complex conjugate of A
$[\mathrm{A}]$	Diagonal matrix of vector A located on the diagonal

Parameters

$\eta_i^{ch}, \eta_i^{dch}$	Charging and discharging efficiency of the battery at i^{th} bus
Δt	time-step
$E_i^{ST,max}$	Rated energy of the battery at bus i
$P_{i,t}^{LD}, Q_{i,t}^{LD}$	Active and reactive power demand at i^{th} bus at time t
$Q_i^{gen,min}, Q_i^{gen,max}$	Minimum and maximum limit of the reactive power capability of the generator at i^{th} bus
Y_{bus}	Admittance matrix of the grid
SOC_i^{min}, SOC_i^{max}	Minimum and maximum limit of the SOC at i^{th} bus
$P_i^{ch,max}, P_i^{dch,max}$	Rated charging and discharging capacity of the battery at i^{th} bus
$\mathcal{V}_i^{min}, \mathcal{V}_i^{max}$	Minimum and maximum limit of the voltage amplitude at i^{th} bus
$C_g, C_b, C_{g,b}$	$n_b \times n_g$ generator, battery, and generator/battery connection matrix

Variables

λ, μ	Lagrange multipliers regarding to equality and inequality constraints
X, x	Set of all variables on the next horizon, set of variables at one time-step
$P_{i,t}^{ch}, P_{i,t}^{dch}$	Charging and discharging power at i^{th} bus at time t
$SOC_{i,t}$	State-of-charge of the battery at i^{th} bus at time t
$V_{i,t}, \mathcal{V}_{i,t}, \delta_{i,t}$	$n_b \times$ 1vectors of complex bus voltages,bus voltage magnitudes and angles at i^{th} bus at time t
$P_{i,t}^{gen}, Q_{i,t}^{gen}$	Active and reactive power production

978-1-5386-5326-5/18/$31.00 2018 IEEE

	from the distributed generator at i^{th} bus at time t

Indices

n_b, n_g, n_l, T	Number of buses, generators, branches, and steps in the next time horizon
i, t	Index of Bus and time
k, l	Number of equality and inequality equations
fr, to	from bus i to j, to bus i from j
v	Number of variables in one time
$-, \sim$	Signs for linear and non-linear equations

I. Introduction

The continuing introduction of renewable energy resources into the power system has already challenged the classical concept of generation, transmission and distribution of electrical power. The optimal operating point of the system changes over time due to the variable generation of intermittent renewable resources. Energy Storage Systems (ESS) can mitigate this variability, but this implies that optimal operating points for the system over an an extended planning horizon are estimated based on forecasted generation. Therefore, development and extension of tools and methods to evaluate and determine possible optimal operating points over multiple time steps is an increasingly important research objective.

One of the most extensively developed and studied methods to estimate the optimal operation point is AC Optimal Power Flow (ACOPF). ACOPF is a nonlinear and non-convex optimization problem, and many different solution proposals have been introduced so far to conditionally handle it, see for instance [1–3] for reviews of historical and recent development. Notable and easily accessible contributions include the OPF functionalities of the open-source MATLAB toolbox MATPOWER[4], including the MATPOWER Interior Point Solver (MIPS)[5]. Interior point methods is one of the most extensively applied methods to solve nonlinear optimisation problems, especially ACOPF problems[6], and briefly put typically involve solving the Karush-Kuhn-Tucker (KKT) conditions using the Newton-Raphson method.

Classical ACOPF gives the optimal operating point only for one time-step. Further extension of ACOPF has led to Multi-period ACOPF (MPOPF), also referred to as Dynamic OPF (DOPF) [7], [8]. In other words, the optimisation problem is extended over time, which in turn incorporates inter-temporal constraints such as storage equations and ramp generator limits. Particularly the recent prospect of large-scale integration of ESSs in power systems has attracted immense interest to research on MPOPF, and we refer to [6] for a review and to e.g. [9] for some more recent developments. Introduction of inter-temporal constraints into the ACOPF problem is a step towards the next generation of ACOPF tool necessitated by the ongoing transformation of the power system. However, the inclusion of inter-temporal constraints also gives rise to new computational challenges. For instance, [10] discusses how the presence of inter-temporal constraints makes the Jacobian of the Newton-Raphson method to become singular and to further lead to the divergence of the solution method. Discussions of the implication of the inter-temporal constraints on the structure of the KKT matrix is discussed in [11] and [9]. Furthermore, most of the DOPF models in the literature are presented relatively compactly and lack a explicit and complete description of the mathematical details of the formulation and the solution method. A few notable examples for single-period OPF are [12] and [13].

Here in this paper, we aim to expand the mathematical formulations of a MPOPF problem explicitly to firstly show that analytical differentiation of the Lagrangian with respect to different variable will reduce the computational cost of the solution method in compare with numerical methods, and secondly to explore the possibility of extension of the method for future research plans. Here, the first and second derivatives of equality and inequality constraints with respect to variables are analytically calculated over the future horizon. The proposed MPOPF solver is compared with MATLAB non-linear solver FMINCON and CONOPT through implementation of a three bus test system in MATLAB and GAMS. The results are presented and discussed to interpret the efficiency of the proposed method.

This paper is organised as follows: section II presents the general formulation of the problem. In section III, we show how to solve the problem though KKT conditions and Newton-Raphson method and finally propose how to calculate the analytical differentiation of the solution proposal. Section IV presents the case study and the interpretation of the numerical results. Finally, we conclude the main results and discuss future work enabled by the development of the proposed solution approach in section V.

II. Formulation of MPOPF

A. General Structure and Formulation

The general formulation of MPOPT consists of an objective function over future horizon and bunch of equality and inequality constraints as it can be seen here:

$$\begin{aligned} &\min_X F(X) \\ &\text{s.t. } G(X) = 0, \\ &\quad\ \ H(X) \leq 0 \end{aligned} \tag{1}$$

where

$$X = \begin{bmatrix} x_1 & x_2 & ... & x_t & ... & x_T \end{bmatrix}^\top \tag{2}$$

and also:

$$x_t = \begin{bmatrix} \delta_t \ \mathcal{V}_t \ P_t \ Q_t \ SOC_t \ P_t^{ch} \ P_t^{dch} \end{bmatrix}^\top_{1\times v} \tag{3}$$

$g(x)$ is the vector of equality and $h(x)$ is the vector of inequality constraints and both of them include linear and non-linear equations shown with $-$ and $\sim$ in the following equation respectively:

$$G(X) = \begin{bmatrix} \widetilde{g}(x_{t=1}) \\ \widetilde{g}(x_{t=2}) \\ \vdots \\ \widetilde{g}(x_{t=T}) \\ \overline{g}(x_{t=1}) \\ \overline{g}(x_{t=2}) \\ \vdots \\ \overline{g}(x_{t=T}) \end{bmatrix}_{k\times 1} \quad H(X) = \begin{bmatrix} \widetilde{h}(x_{t=1}) \\ \widetilde{h}(x_{t=2}) \\ \vdots \\ \widetilde{h}(x_{t=T}) \\ \overline{h}(x_{t=1}) \\ \overline{h}(x_{t=2}) \\ \vdots \\ \overline{h}(x_{t=T}) \end{bmatrix}_{l\times 1} \tag{4}$$

B. Detail of Objective Function and Constraints:

1) Objective Function:
Objective function is simply minimization of costs for all generators over time horizon of T.

$$F(X) = \sum_{t=1}^{T} \sum_{i=1}^{n_g} f(P_{t,i}^{gen}) \tag{5}$$

If we assume all generators are modeled by a quadratic function, then objective function can be written as:

$$\min_X \sum_{t=1}^{T} \left(\sum_{i=1}^{n_g} a_i {P^{gen}}^2_{i,t} + b_i P_{i,t}^{gen} + c_i \right) \tag{6}$$

2) Power Flow:
Using rectangular coordinates, voltage and power injection matrices V, S_{bus} (rectangular coordinate is used to ease the process of taking differentiation) can be written as:

$$V_{i,t} = V_{di,t} + jV_{qi,t} \tag{7}$$

$$I_{bus,t} = Y_{bus} V_t \tag{8}$$

$$S_{bus,t} = V_t . I_{bus,t}^* = V_t . Y_{bus} . V_t^* \tag{9}$$

Consider the power balance equation:

$$\widetilde{g}(x_t) = S_{bus,t} + S_{d,t} - C_{g,b} S_{g,t} = 0 \tag{10}$$

C. Voltage magnitude and angle Constraints

Upper and lower bounds of voltages magnitude and angles are defined with constraints 13 and 14. The voltage angle for slack bus is set to be zero.

$$\mathcal{V}_i^{min} \leq \mathcal{V}_{i,t} \leq \mathcal{V}_i^{max} \tag{13}$$

$$\delta_i^{min} \leq \delta_{i,t} \leq \delta_i^{max} \quad \forall i \neq slack \quad \& \quad \delta_{slack} = 0 \tag{14}$$

D. Line Constraints

If we take $(S^{max})^2$ as the squared vector of apparent power flow limits, then flow constraints, the non-linear part of H(X) for one time-step, can be written as:

$$[\widetilde{h}_t] = \begin{bmatrix} h_t^{fr} \\ h_t^{to} \end{bmatrix} = \begin{bmatrix} [S^{fr^*}] S^{fr} - (S^{max})^2 \\ [S^{to^*}] S^{to} - (S^{max})^2 \end{bmatrix} \leq 0 \tag{15}$$

where $S^{fr} = P^{fr} + jQ^{fr}$.

E. Storage Constraints

The storage model used here is a linear storage model including charge, discharge and SOC variables. We neglect the self-discharge and battery degradation over the next optimisation horizon.

$$\begin{aligned} 0 \leq P_{i,t}^{ch} \leq P_i^{ch,max} \\ 0 \leq P_{i,t}^{dch} \leq P_i^{dch,max} \end{aligned} \tag{16}$$

$$SOC_i^{min} \leq SOC_i(t) \leq SOC_i^{max} \tag{17}$$

$$SOC_{i,t} = \frac{E_{i,t}^{ST}}{E_i^{ST,max}} \tag{18}$$

$$\begin{aligned} &E_{i,t}^{ST} = \\ &\quad E_{i,t-1}^{ST} + \eta_i^{ch} P_{i,t}^{ch} \Delta t - \frac{P_{i,t}^{ch} \Delta t}{\eta_i^{dch}} \end{aligned} \tag{19}$$

III. Solution Proposal

A. Primal-Dual Interior Point

The problem formulated in the last section can be solved using primal-dual interior method mainly inspired from [5]. Converting the inequality equations to equality in (1) then we get:

$$\begin{aligned} &\min_X \left[F(X) - \gamma \sum_{n=1}^{l} ln(Z_n) \right] \\ &\text{s.t. } G(X) = 0, \\ &H(X) + Z = 0 \end{aligned} \tag{20}$$

and Lagrangian of the formulated problem (1) becomes:

$$\begin{aligned} \mathcal{L}^{\gamma}(X, Z, \lambda, \mu) &= f(X) + \lambda^\top G(X) \\ &+ \mu^\top (H(X) + Z) - \gamma \sum_{n=1}^{l} ln(Z_n) \end{aligned} \tag{21}$$

To write Karush-Kuhn-Tucker (KKT) conditions, partial differentials of (21) can be extracted with respect to the all the variables:

$$\begin{aligned} \mathcal{L}_X^{\gamma}(X, Z, \lambda, \mu) &= f_X + \lambda^\top G_X + \mu^\top H_X \\ \mathcal{L}_Z^{\gamma}(X, Z, \lambda, \mu) &= \mu^\top - \gamma e^\top [Z]^{-1} \\ \mathcal{L}_\lambda^{\gamma}(X, Z, \lambda, \mu) &= G^\top (X) \\ \mathcal{L}_\mu^{\gamma}(X, Z, \lambda, \mu) &= H^\top (X) + Z^\top \end{aligned} \tag{22}$$

and the Hessian of the Lagrangian with respect to X can be written as:

$$\mathcal{L}_{XX}^{\gamma}(X, Z, \lambda, \mu) = f_{XX} + G_{XX}(\lambda) + H_{XX}(\mu) \tag{23}$$

$$\begin{aligned} &F(X, Z, \lambda, \mu) = \begin{bmatrix} f_X + \lambda^\top G_X + \mu^\top H_X \\ \mu^\top - \gamma e^\top [Z]^{-1} \\ G^\top (X) \\ H^\top (X) + Z^\top \end{bmatrix} = 0 \\ &Z > 0 \\ &\mu > 0 \end{aligned} \tag{24}$$

Using Newton-Raphson's method to solve equation (24) and some simplification, it can finally be written:

$$\begin{bmatrix} M & G_X^\top \\ G_X & 0 \end{bmatrix} = \begin{bmatrix} \Delta X \\ \Delta \lambda \end{bmatrix} = \begin{bmatrix} -N \\ -G_X \end{bmatrix} \tag{25}$$

In (25) M and N are defined as:

$$\begin{aligned} M &= f_{XX} + G_{XX}(\lambda) + H_{XX}(\mu) + H_X^\top [Z]^{-1} [\mu] H_X \\ N &= f_X^\top + G_X^\top \lambda + H_X^\top \mu + H_X^\top [Z]^{-1} (\gamma e + [\mu] H(X)) \end{aligned} \tag{26}$$

$$\overbrace{\left[P_{i,t}^{gen}+P_{i,t}^{SDch}-P_{i,t}^{SCh}\right]}^{\Re[C_{g,b}S_{g,t}]}-\overbrace{\left[P_{i,t}^{LD}\right]}^{\Re[S_{d,t}]}=\overbrace{\sum_{i=1}^{N}\left[V_{di,t}(G_{ik}V_{dk,t}-B_{ik}V_{qk,t})\qquad+V_{qi,t}(B_{ik}V_{dk,t}+G_{ik}V_{qk,t})\right]}^{\Re[S_{bus,t}]} \tag{11}$$

$$\overbrace{Q_{i,t}^{gen}}^{\Im[C_gS_{g,t}]}-\overbrace{Q_{i,t}^{LD,t}}^{\Im[S_{d,t}]}=-\overbrace{\sum_{i=1}^{N}\left[-V_{di,t}(B_{ik}V_{dk,t}-G_{ik}V_{qk,t})\qquad+V_{qi,t}(G_{ik}V_{dk,t}-B_{ik}V_{qk,t})\right]}^{\Im[S_{bus,t}]} \tag{12}$$

Solving (25) numerically results to the locally optimum point X^*. The detail of numerical solution in Newton's method can be seen in [5].

B. Analytical Derivatives

In this section the first and second derivatives of $H(X)$, $G(X)$ and $F(X)$ will be extracted. In general, if we assume a complex scalar function $f:\mathbb{R}^n\to\mathbb{C}$ of a real vector such as (2), the first derivative can be calculated as:

$$f_X=\frac{\partial f}{\partial X}=\left[\frac{\partial f}{\partial x_1}\quad\frac{\partial f}{\partial x_2}\quad...\quad\underbrace{\frac{\partial f}{\partial x_t}}_{\Downarrow}\quad...\quad\frac{\partial f}{\partial x_T}\right]$$
$$\left[\frac{\partial f}{\partial\delta_t}\ \frac{\partial f}{\partial V_t}\ \frac{\partial f}{\partial P_t}\ \frac{\partial f}{\partial Q_t}\ \frac{\partial f}{\partial(SOC_t)}\ \frac{\partial f}{\partial P_t^{ch}}\ \frac{\partial f}{\partial P_t^{dch}}\right] \tag{27}$$

$$f_{XX}=\frac{\partial^2 f}{\partial X^2}=\frac{\partial}{\partial X}\left(\frac{\partial f}{\partial X}\right)^\top=\begin{bmatrix}\frac{\partial^2 f}{\partial x_1^2} & \cdots & \frac{\partial^2 f}{\partial x_1x_n}\\ \vdots & \ddots & \vdots\\ \frac{\partial^2 f}{\partial x_nx_1} & \cdots & \frac{\partial^2 f}{\partial x_n^2}\end{bmatrix} \tag{28}$$

Eqs. (27) and (28) are the basic forms of first and second derivatives of objective function which is $f:\mathbb{R}^n\to\mathbb{C}$. However, constraints G(X) and H(X) are complex vector functions $f:\mathbb{R}^n\to\mathbb{C}^m$ and therefore:

$$G(X)=\begin{bmatrix}g_1(X) & g_2(X) & \dots & g_k(X)\end{bmatrix}^\top_{1\times k} \tag{29}$$

First derivative of this complex vector function can be written as:

$$G_X=\frac{\partial G}{\partial X}=\begin{bmatrix}\frac{\partial g_1}{\partial x_1} & \cdots & \frac{\partial g_1}{\partial x_t} & \cdots & \frac{\partial g_1}{\partial x_T}\\ \vdots & \ddots & \vdots & \ddots & \vdots\\ \frac{\partial g_k}{\partial x_1} & \cdots & \frac{\partial g_k}{\partial x_t} & \cdots & \frac{\partial g_k}{\partial x_T}\end{bmatrix}_{k\times(T.v)} \tag{30}$$

$$H_X=\frac{\partial H}{\partial X}=\begin{bmatrix}\frac{\partial h_1}{\partial x_1} & \cdots & \frac{\partial h_1}{\partial x_t} & \cdots & \frac{\partial h_1}{\partial x_T}\\ \vdots & \ddots & \vdots & \ddots & \vdots\\ \frac{\partial h_l}{\partial x_1} & \cdots & \frac{\partial h_l}{\partial x_t} & \cdots & \frac{\partial h_l}{\partial x_T}\end{bmatrix}_{l\times(T.v)} \tag{31}$$

Second derivative of G(X) and H(X) is only required to calculate the Hessian of the Lagrangian, Eq. (23). Calculation of second derivatives might be a bit confusing since 3D set of partial derivatives will not be calculated here [12]. The reason fairly simple and straightforward. In this context, we are using a Newton-Raphson method to find where the partials of a Lagrangian are equal to zero. It is the Hessian of the Lagrangian function in (21) that we need to compute and we always compute it with a known lambda vector. Therefore, its only the partial with respect to X of the vector resulting from multiplying the transpose of the Jacobian by lambda that is needed in this context, which means:

$$G_{XX}=\frac{\partial}{\partial X}(G_X^\top\lambda) \tag{32}$$

$$G_{XY}=\frac{\partial}{\partial Y}(G_X^\top\lambda) \tag{33}$$

The same types of derivatives can be written for $H(X)$ too. More details regarding the first and second partial differentials of $F(X)$, $G(X)$ and $H(X)$, and their matrices will be discussed in the future work.

C. Jacobian of the Newton-Raphson Method

Fig. 1 shows the non-zero part of Jacobian of Newton-Raphson's Method on Eq.(25) where $T=2$. As it can be seen, M is constructed from two large squares which specifically comes from summation of $G_{XX}(\lambda)$, $H_{XX}(\mu)$ and $H_X^\top H_X$ and the diagonal line is summation of F_{XX} and a part that comes from interaction of $[Z]^{-1}[\mu]$ (inverse diagonal of slack variables times diagonal of Lagrangian of inequality constraints) in the following mathematical operations: $H_X^\top[Z]^{-1}[\mu]H_X$. G_X is formed from two large squares too, which are first derivatives of power flow equations w.r.t variables. Block A represents the equality equations regarding the grid constraints, and B stands for the Inter-temporal constraints that are related to storage equations.

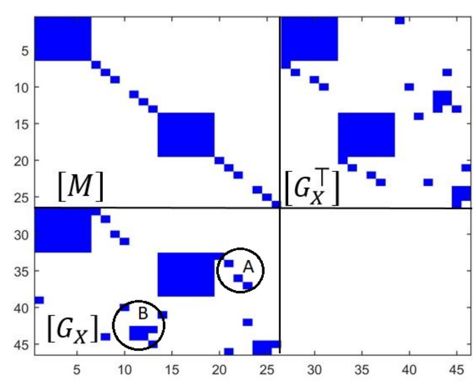

Fig. 1. Structure of Jacobian of the Newton-Raphson's algorithm for two timesteps, refer to Eq. (25)

IV. Case Study and Numerical Results

For the purpose of efficiency evaluation of the proposed MPOPF, we used a very simple 3 bus case study shown in

Fig. 2 which consists of a generator on bus 1, a battery on bus 2 and load on bus 3. The simulation time horizon is selected two for the sake of simplicity. Fig. 3 shows the variation of base load within two time-steps. With the assumption that the generator has a quadratic cost function and no costs over battery operation; therefore, optimal dispatch of generator, P_g, is to charge the battery at the first time and discharge the saved energy on the second time as it can be observed in Fig. 3. Fig. 4 shows the charge, discharge and stored energy of the battery within the same time horizon. As expected and discussed, since the battery operation cost is zero; therefore, battery charges at the first time-step and discharges on the second one to flatten the overall generation unit profile within two time-step.

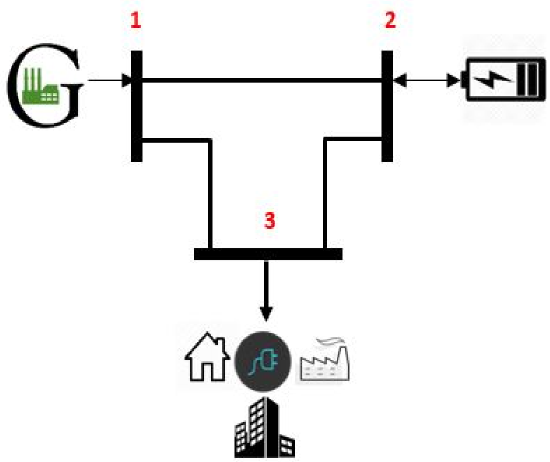

Fig. 2. Three bus case study simulated here in this study

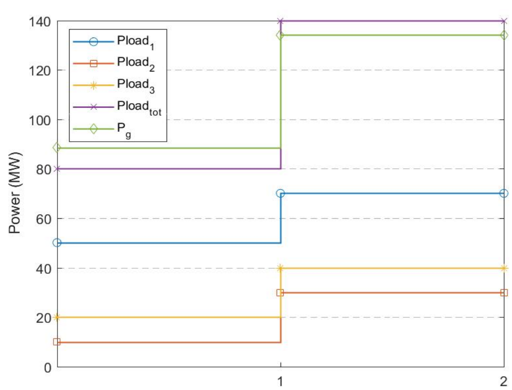

Fig. 3. Base loads and optimal generating power in the 3 bus case study

The case study is also formulated in GAMS and solved with NLP solvers, as listed in II, to compare the computational time and convergence speed. All convergence criteria for commercial solvers are selected to be the default value of each solver in the list. For the sake of comparison, the termination tolerances for the proposed algorithm can be seen in Table I. Definition and formulation of feasibility, complementary, gradient and cost conditions can be found in [5]. and These codes ran on the same PC with Intel 2.7 GHz Core i7 CPU. Table II represents the computational time comparison

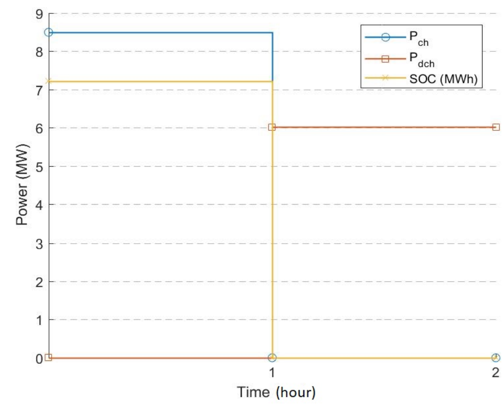

Fig. 4. Charge, discharge and SOC of battery with two time-steps, charging at the first time and discharging on the second one.

between all used solvers with exactly the same implemented formulations. All the numerical parameters are the same for each simulation on table II and consequently optimal solutions converged to the same objective value (the same optimal point).

As it is shown, the computational convergence time for the proposed solution method is almost 10 times less than the commercial solvers. The main reason here is to use the analytical derivatives of f_X,G_X, H_X, f_{XX}, G_{XX} and H_{XX} when Eq. 26 is calculated. However, commercial solvers use numerical methods to calculate derivatives regarding the NLP problem.

TABLE I. TERMINATION TOLERANCES FOR THE PROPOSED MPOPF

Criterion	Value ($\times E - 10$)
feasibility condition	1.0
complementarity condition	1.0
gradient condition	1.0
cost condition	1.0

TABLE II. COMPUTATIONAL TIME FOR DIFFERENT SOLVERS AND WITH THE SAME CONVERGENCE CRITERIA

Implemented environment	Solver	Computational time (sec)
MATLAB	FMINCON	0.411
GAMS	CONOPT	0.408
GAMS	CONOPT4	0.592
GAMS	COUENNE	0.637
GAMS	IPOPT	0.538
GAMS	IPOPTH	0.517
GAMS	KNITRO	0.461
GAMS	MINOS	0.413
GAMS	PATHNLP	0.472
GAMS	SNOPT	0.385
MATLAB	The Proposed Method	0.056

V. CONCLUSION AND FUTURE WORK

A solution method of multi-period ACOPF based on primal-dual interior point method is proposed in this paper. Firstly, the method has been introduced and partial derivatives of linear and non-linear constraints, objective function, and KKT condition have been explored analytically. Secondly, a simple three bus case study has been solved through the proposed solution method. Finally, the same formulation has been implemented in GAMS and solved with different solvers to compare the convergence time. The computational cost of the proposed method is compared with different commercial solvers to assess the computational efficiency of the proposed method.

In future work, the Authors are planning to a) expand the analytical differentiation for new constraints and objective function into the current formulations, b) explore Jacobian singularities in Newton-Raphson's method and try to avoid it c) use the automatic differentiation instead of analytical to explore the possibility of computational efficiency improvements.

ACKNOWLEDGMENT

The authors acknowledge Iver Bakken Sperstad for his comments and discussions on this work.

REFERENCES

[1] S. Frank, I. Steponavice, and S. Rebennack, "Optimal power flow: A bibliographic survey i formulations and deterministic methods," *Energy Systems*, vol. 3, no. 3, p. 221258, 2012.

[2] ——, "Optimal power flow: A bibliographic survey ii non-deterministic and hybrid methods," *Energy Systems*, vol. 3, no. 3, p. 259289, 2012.

[3] F. Capitanescu, "Critical review of recent advances and further developments needed in ac optimal power flow," *Electric Power Systems Research*, vol. 136, p. 5768, 2016.

[4] R. D. Zimmerman, C. E. Murillo-Sanchez, and R. J. Thomas, "MATPOWER: Steady-State Operations, Planning, and Analysis Tools for Power Systems Research and Education," *IEEE Transactions on Power Systems*, vol. 26, no. 1, pp. 12–19, Feb. 2011.

[5] H. Wang, C. E. Murillo-Sanchez, R. D. Zimmerman, and R. J. Thomas, "On Computational Issues of Market-Based Optimal Power Flow," *IEEE Transactions on Power Systems*, vol. 22, no. 3, pp. 1185–1193, Aug. 2007.

[6] I. B. Sperstad and H. Marthinsen, "Optimal power flow methods and their application to distribution systems with energy storage - a survey of available tools and methods," SINTEF Energy Research, Report TR A7604, 2016. [Online]. Available: hdl.handle.net/11250/2432401

[7] M. E. El-Hawary and D. H. Tsang, "The Hydrothermal Optimal Load Flow, A Practical Formulation and Solution Techniques Using Newton's Approach," *IEEE Transactions on Power Systems*, vol. 1, no. 3, pp. 157–166, Aug. 1986.

[8] H. Wei, H. Sasaki, J. Kubokawa, and R. Yokoyama, "Large scale hydrothermal optimal power flow problems based on interior point nonlinear programming," *IEEE Transactions on Power Systems*, vol. 15, no. 1, pp. 396–403, Feb. 2000.

[9] D. Kourounis, A. Fuchs, and O. Schenk, "Towards the Next Generation of Multiperiod Optimal Power Flow Solvers," *IEEE Transactions on Power Systems*, vol. PP, no. 99, pp. 1–1, 2018.

[10] K. Baker, G. Hug, and X. Li, "Inclusion of inter-temporal constraints into a distributed Newton-Raphson method," in *2012 North American Power Symposium (NAPS)*, Sep. 2012, pp. 1–6.

[11] N. Meyer-Huebner, M. Suriyah, and T. Leibfried, "On efficient computation of time constrained optimal power flow in rectangular form," in *2015 IEEE Eindhoven PowerTech*, Jun. 2015, pp. 1–6.

[12] R. D. Zimmerman, "Ac power flows, generalized opf costs and their derivatives using complex matrix notation," 2010.

[13] S. Frank and S. Rebennack, "An introduction to optimal power flow: Theory, formulation, and examples," *IIE Transactions*, vol. 48, no. 12, pp. 1172–1197, 2016. [Online]. Available: https://doi.org/10.1080/0740817X.2016.1189626

VI. APPENDIX

Details regarding the case study are listed in tables V-III Some simulation parameters:
$SOC_0 = 0.00$
$\eta_{chrg,i} = 0.85$
$\eta_{dischrg,i} = 1.2$

TABLE III. UPPER BOUND AND LOWER BOUND OF ALL VARIABLES IN ONE TIME STEP

-	δ_1	δ_2	δ_3	
LB	0.00	-3.14	-3.14	
UB	0.00	3.14	3.14	
-	V_3	V_3	V_3	
LB	0.90	0.90	0.90	
UB	1.10	1.10	1.10	
	P_1	P_{bat}	Q_1	Q_{bat}
LB	0.00	-0.50	-1.00	0.00
UB	3.00	0.50	1.00	0.00
	$P_{SCh,t}$	$P_{SDch,t}$	SOC	
LB	0.00	0.00	0.00	
UB	0.50	0.50	3.00	

TABLE IV. BRANCH DATA

From Bus	To Bus	r	x	b
1	2	0.01008	0.0504	0.1025
1	3	0.00744	0.0372	0.0775
3	2	0.00744	0.0372	0.0775

TABLE V. GENERATORS COEFFICIENTS

time	a	b	c
t_1	0.11	5	550
t_2	0.11	5	550

TABLE VI. BASE LOAD IN DIFFERENT TIME STEPS

Bus number	P_{d1}	P_{d2}
1	50	70
2	10	30
3	20	40

TABLE VII. BASE LOAD IN DIFFERENT TIME STEPS

Bus number	Q_{d1}	Q_{d2}
1	50	50
2	10	10
3	20	20